Title: Myosin IIA is essential for *Shigella flexneri* cell-to-cell spread

Authors: Mabel Lum and Renato Morona*

Address: School of Molecular and Biomedical Science, University of Adelaide, Adelaide, South Australia, Australia

Contact details:

* E-mail: renato.morona@adelaide.edu.au

Tel: 61 8 8313 4151

Fax: 61 8 8313 7532

Abstract

A key feature of *Shigella* pathogenesis is the ability to spread from cell to cell post invasion. This is dependent on the bacteria's ability to initiate *de novo* F-actin tail polymerisation, followed by protrusion formation, uptake of bacteria-containing protrusion and finally lysis of the double membrane vacuole in the adjacent cell. In epithelial cells cytoskeletal tension is maintained by the actin-myosin II networks. In this study, the role of myosin II and its specific kinase, myosin light chain kinase (MLCK) during *Shigella* intercellular spreading was investigated in HeLa cells. Inhibition of MLCK and myosin II, as well as myosin IIA knockdown significantly reduced *Shigella* plaque and infectious focus formation. Protrusion formation and intracellular bacterial growth was not affected. Low levels of myosin II were localised to the *Shigella* F-actin tail. HeLa cells were also infected with *Shigella* strains defective in cell-to-cell spreading. Unexpectedly loss of myosin IIA labelling was observed in HeLa cells infected with these mutant strains. This phenomenon was not observed with WT *Shigella* or with the less abundant myosin IIB isoform, suggesting a critical role for myosin IIA.

Introduction

Shigella flexneri is the causative agent of bacillary dysentery (shigellosis). Post ingestion, *Shigella* bacteria invade the host intestinal epithelium via microfold cells. Resident macrophages in the follicle-associated epithelium undergo cell death (pyroptosis) induced by *Shigella* through caspase-1 activation, which releases interleukin-1β and interleukin-18 (Zychlinsky *et al.*, 1992; Sansonetti *et al.*, 2000; Senerovic *et al.*, 2012). Interleukin-1β induces a strong inflammatory response and interleukin-18 magnifies innate immune responses (Sansonetti *et al.*, 2000). After *Shigella* are released into the basolateral compartment, *Shigella* invade enterocytes via the type three secretion system, followed by lysis of the endocytic vacuole and replication in the host cytoplasm (Sansonetti *et al.*, 1986; Cossart & Sansonetti, 2004). Concurrently the *Shigella* IcsA (VirG) protein interacts with the host Neural Wiskott-Aldrich syndrome protein (N-WASP) and Arp2/3 complex to initiate *de novo* F-actin nucleation and polymerisation, leading to actin-based motility (ABM) (Bernardini *et al.*, 1989; Suzuki *et al.*, 1998; Rohatgi *et al.*, 1999).

ABM facilitates *Shigella* intracellular movement and intercellular spreading into neighbouring cells via protrusion formation. After escaping from the double membrane vacuole, subsequent

cycles of infection are initiated (Schuch *et al.*, 1999). *Shigella* ABM is dependent on IcsA, an outer membrane protein, and lipopolysaccharide (LPS) found on the bacterial surface (Makino *et al.*, 1986; Bernardini *et al.*, 1989; Lett *et al.*, 1989). IcsA is necessary for pathogenesis as Δ*icsA* strains have attenuated virulence in human volunteers and in animal infection models (Makino *et al.*, 1986; Kotloff *et al.*, 1996; Sansonetti *et al.*, 1999). Smooth (WT) *Shigella* strains express the complete LPS molecule, i.e. the lipid A core, core oligosaccharide and O-antigen subunit. In rough LPS strains the O-antigen subunit is absent due to mutations in chromosomal genes encoding LPS synthesis. Rough strains can invade epithelial cells and initiate ABM but have a defect in cell-to-cell spreading (Okamura *et al.*, 1983; Hong & Payne, 1997; Van Den Bosch *et al.*, 1997).

Enterocytes, the site of *Shigella* infection, are polarised colonic epithelial cells characterised by apical junctional complexes, consisting of tight junctions and adherens junctions at the most apical end, which are undercoated with a prominent network of actin-myosin II (actomyosin) ring (Miyoshi & Takai, 2005). For cell-to-cell spreading to occur, the tensions of the actomyosin ring have to be overcome before disruption of the cellular contacts can take place (Rajabian *et al.*, 2009). *Shigella* engulfment, but not protrusion formation into the neighbouring cell is triggered by phosphoinositide 3-kinase and is dependent upon dynamin II, Epsin-1 and clathrin, components of the clathrin-mediated endocytic pathway (Fukumatsu *et al.*, 2012; Lum *et al.*, 2013). Adherens junction and tight junction components such as L-CAM, α-catenin, β-catenin, α-actinin and vinculin localise to the *Shigella* actin tail during protrusion formation. L-CAM is crucial for cell-to-cell spread as it helps to maintain a tight association between the bacterium and the membrane of the protrusions (Kadurugamuwa *et al.*, 1991; Sansonetti *et al.*, 1994). Knockdown of myosin-X, a component of adherens junctions, resulted in shortened and thickened protrusion stalks which reduced *Shigella*'s ability to form plaques (Bishai *et al.*, 2012). *Shigella* invasion and dissemination is also dependent on ATP release by connexin 26, and formins, Dia1 and Dia2 (Tran Van Nhieu *et al.*, 2003; Heindl *et al.*, 2009). Similar to the Arp2/3 complex, formins initiate *de novo* actin polymerisation but also crosslink actin filaments (Esue *et al.*, 2008).

In an attempt to identify host proteins which are differentially recruited to rough and smooth LPS *Shigella* strains, localisation of various proteins to the F-actin tail and bacterial cells inside infected HeLa cells were carried out by immunofluorescence (IF) microscopy with a panel of antibodies. Curiously it was observed that non-muscle myosin IIA (myosin IIA), but not IIB protein levels were significantly reduced in HeLa cells infected with rough LPS (R-LPS) and Δ*icsA* strains. The involvement of myosin and its specific kinase, myosin light chain kinase (MLCK) has previously been reported at different stages of *Shigella* infection. MLCK and myosin II were previously implicated in *Shigella* cell-to-cell spread in Caco-2 cells (Rathman *et al.*, 2000). In a later study Mostowy *et al.* (2010) showed that in HeLa cells, myosin II was recruited to the septin cage which entraps intracytosolic *Shigella* without F-actin tails and targets the bacterium to the autophagy pathway for degradation.

In this study, treatment of HeLa cells with MLCK and myosin II inhibitors, as well as siRNA knockdown of myosin IIA heavy chain (*MYH9*) reduced *Shigella* infectious focus and plaque formation. No effect on intracellular bacterial growth and bacteria protrusion formation were observed. Low levels of myosin IIA were also localised to the *Shigella* F-actin tail. Indirect protein quantification with fluorescence labelling showed that myosin IIA, but not IIB protein levels decreased by ~50% in a subpopulation of HeLa cells infected with Δ*icsA* and R-LPS *Shigella* strains which are defective in cell-to-cell spreading. Furthermore a significantly greater proportion of HeLa cells infected with the *Shigella* Δ*icsA*, R-LPS double mutant had reduced myosin IIA compared to Δ*icsA* or R-LPS-infected HeLa cells, suggesting a synergistic effect between the IcsA and LPS defects.

Materials and methods

Bacterial strains and growth media

The strains used in this study are listed in Table 1. *S. flexneri* strains were grown from a Congo Red positive colony as described previously (Morona *et al.*, 2003) and were routinely cultured in Luria Bertani (LB) broth and on LB agar. Bacteria were grown in media for 16 h with aeration, subcultured 1/20 and then grown to mid-exponential growth phase by incubation with aeration for 1.5 h at 37°C. Where appropriate, media were supplemented with tetracycline (4 or 10 μg mL^{-1}) or kanamycin (50 μg mL^{-1}).

Chemicals and antibodies

(-)-Blebbistatin (50 mM stock - 203391; Merck Calbiochem), (+)-blebbistatin (50 mM stock - 203392; Merck Calbiochem), ML-7 (30 mM stock - I2764; Sigma-Aldrich) and ML-9 (100 mM stock - C1172; Sigma-Aldrich) were prepared in dimethyl sulfoxide (DMSO) (D2650; Sigma-Aldrich). Rabbit anti-Myosin IIA (M8064; Sigma-Aldrich) and rabbit anti-GAPDH antibodies (600-401-A33; Rockland Immunochemicals, Inc.) were used at 1:400 and 1:3000 for Western immunoblotting, respectively. For immunofluorescence (IF) microscopy, rabbit anti-Myosin IIA, rabbit anti-Myosin IIB (M7939; Sigma-Aldrich) and Alexa 594-conjugated donkey anti-rabbit secondary antibodies (Molecular Probes) were used at 1:100.

Reverse transfection and HeLa cell lysate preparation

MYH9 (Myosin IIA) siRNA (L-007668-00-0005) and siRNA controls (Non-targeting Pool; D-001810-10-05, siGLO Green Transfection Indicator; D-001630-01-05) were purchased from Thermo Scientific. siRNAs were transfected with DharmaFECT 3 Transfection Reagent (T-2003-03) and DharmaFECT Cell Culture Reagent (DCCR; B-004500-100), also purchased from Thermo Scientific. Reverse transfection of HeLa cells (Human, cervical, epithelial cells ATCC #CCL-70) were carried out based on a method by Thermo Scientific. siRNA were prepared as a 5 µM stock and the final concentration used was 50 nM. HeLa cells were transfected and HeLa cell lysate were prepared as described previously (Lum *et al.*, 2013).

SDS-PAGE and Western immunoblotting

SDS-PAGE (12% acrylamide gel) and Western immunoblotting were carried out as described previously (Lum *et al.*, 2013). Molecular weight markers used were BenchMark™ Pre-Stained Protein Ladder (Invitrogen).

Plaque assay

Plaque assays were performed with HeLa cells as described previously (Oaks *et al.*, 1985) with modifications. 1.2×10^6 HeLa cells were seeded in six-well trays in minimal essential medium (MEM), 10% FCS, 1% penicillin/streptomycin. Cells were grown to confluence overnight and were washed twice with Dulbecco's modified Eagle medium (DMEM) prior to inoculation. 2.5 ×

10^4 mid-exponential phase bacteria were added to each well. Trays were incubated at 37°C, 5% CO_2 and were rocked gently every 15 min to spread the inoculum evenly across the well. At 90 min post infection, the inoculum was aspirated. 3 mL of the first overlay (DMEM, 5% FCS, 20 µg mL^{-1} gentamicin, 0.5% (w/v) agarose [Seakem ME]) was added to each well. ML-7, ML-9 or DMSO were added and were swirled to ensure even distribution. The second overlay (DMEM, 5% FCS, 20 µg mL^{-1} gentamicin, 0.5% (w/v) agarose, 0.1% (w/v) Neutral Red solution [Gibco BRL]) was added 48 h post infection and plaques were imaged 6 h later. All observable plaques were counted and the diameter was measured for each condition in each experiment. At least 50 plaques were measured for each condition.

Infectious focus assay

1.2×10^6 HeLa cells were seeded in six-well trays in MEM, 10% FCS, 1% penicillin/streptomycin. Cells were grown to confluence overnight and were washed twice with DMEM prior to inoculation. 5×10^4 mid-exponential phase bacteria expressing mCherry were added to each well. Trays were incubated at 37°C, 5% CO_2 and were rocked every 15 min to spread the inoculum evenly across the well. At 90 min post infection, the inoculum was aspirated. 1.5 mL of DMEM (phenol red-free) (31053-028; Life Technologies), 1 mM sodium pyruvate, 5% FCS, 20 µg mL^{-1} gentamicin, 2 mM IPTG was added to each well. (+)-Blebbistatin, (-)-blebbistatin or DMSO were added and were swirled to ensure even distribution. 24 h later the infectious foci were imaged with an Olympus IX-70 microscope using a 10× objective. The filter set used was DA/FI/TX-3X-A-OMF (Semrock). Fluorescence and phase contrast images were captured and false colour merged with the Metamorph software program (Version 7.7.3.0, Molecular Devices). The area of the infectious focus, i.e. area where mCherry was expressed, was outlined and measured with Metamorph. All observable infectious foci were counted and the area was measured for each condition in each experiment. At least 15 infectious foci were measured for each condition. The following modifications were made for transfected cells. HeLa cells were transfected prior to infectious focus assay as described previously in 12-well trays (Lum *et al.*, 2013). On day 3, the infectious focus assay was carried out. Transfected HeLa cells were washed twice with DMEM prior to inoculation. 5×10^4 mid-exponential phase bacteria expressing mCherry were added to each well.

Invasion assay and immunofluorescence (IF) microscopy

HeLa cells (8×10^4) were seeded onto sterile glass cover slips in 24-well trays in MEM, 10% FCS, 1% penicillin/streptomycin. For transfected cells, HeLa cells were transfected as described previously (Lum *et al.*, 2013). Cells were grown to semi-confluence overnight, washed twice with Dulbecco's PBS (D-PBS) and once with MEM, 10% FCS. 4×10^7 mid-exponential phase bacteria were added to each well and subsequently centrifuged (2,000 rpm, 7 min, Heraeus Labofuge 400 R) onto HeLa cells. After 1 h incubation at 37°C, 5% CO_2, the infected cells were washed thrice with D-PBS and incubated with 0.5 mL MEM containing 40 µg mL^{-1} gentamicin for a further 1.5 h (or 3.5 h for labelling with anti-activated caspase 3). Infected cells were washed thrice in D-PBS, fixed in 3.7% (v/v) formalin for 15 min, incubated with 50 mM NH_4Cl in D-PBS for 10 min, followed by permeabilisation with 0.1% Triton X-100 (v/v) for 5 min. After blocking in 10% FCS in PBS, the infected cells were incubated at 37°C for 30 min with the desired primary antibody. After washing in PBS, coverslips were incubated with Alexa 594-conjugated donkey anti-rabbit secondary antibody (Molecular Probes) (1:100). F-actin was visualised by staining with Alexa Fluor 488-conjugated phalloidin (2 U mL^{-1}) and 4',6'-diamidino-2-phenylindole (DAPI) (10 µg mL^{-1}) was used to counterstain bacteria and HeLa cell nuclei. Coverslips were mounted on glass slides with Mowiol 4-88 (Calbiochem) containing 1 µg mL^{-1} *p*-phenylenediamine (Sigma) and was imaged using a 100× oil immersion objective (Olympus IX-70). The filter set used was DA/FI/TX-3X-A-OMF (Semrock). Fluorescence and phase contrast images were false colour merged using the Metamorph software program.

Indirect quantification of protein levels by IF

Indirect immunofluorescence was quantified with Metamorph to determine protein levels in bacteria-infected HeLa cells compared to uninfected HeLa cells. ***"Invasion assay and IF microscopy"*** was carried out as described above. Cells were imaged with a 40× objective. In each image, the maximum fluorescence (100%) was determined by the mean fluorescence of uninfected HeLa cells (2 - 3 cells). Infected and uninfected cells were selected by tracing and the mean fluorescence of the outlined area was determined with Metamorph. HeLa cells exhibited two distinct immunofluorescence staining patterns (high and low) when infected compared to uninfected HeLa cells. In such instances, the HeLa cells were arbitrarily assigned into distinct

populations, before the level of fluorescence of the infected cell was determined. The fluorescence of ≥ 100 infected cells for each category was measured for each experiment.

Protrusion formation

HeLa cells were seeded, infected and fixed as per *"**Invasion assay and IF microscopy**"*. HeLa cells were washed twice with 1× Annexin V binding buffer (99902; Biotium) prepared in milliQ (18.2 MΩ·cm) water, mounted on glass slides with the same buffer and were imaged using a 40× oil immersion phase contrast objective (Olympus IX-70). Protrusion formation was defined as any extensions of bacterial projection(s) (minimum of a full bacterial length) beyond the periphery of the HeLa cell. For each condition in each experiment, a minimum of 100 cells were imaged.

Assay for growth of intracellular bacteria

HeLa cells (8×10^4) were seeded in 24-well trays in MEM, 10% FCS, 1% penicillin/streptomycin. Cells were grown to semi-confluence overnight, washed twice with D-PBS and once with MEM, 10% FCS. 4×10^7 mid-exponential phase bacteria were added to each well (multiplicity of infection ~500). The bacteria were centrifuged (2,000 rpm, 7 min, Heraeus Labofuge 400 R) onto HeLa cells. After 1 h incubation at 37°C, 5% CO_2, the infected cells were washed thrice with D-PBS and incubated with 0.5 mL MEM containing 40 µg mL^{-1} of gentamicin. At the indicated intervals, monolayers (in duplicate) were washed four times in D-PBS and were lysed with 0.1% (v/v) Triton X-100 in PBS for 5 min and bacteria were enumerated on tryptic soy agar (Gibco) plates.

Statistical analysis

Statistical analysis was carried out using GraphPad Prism 6. Results are expressed as means ± SEM of data obtained in independent experiments. Statistical differences between three or more groups were determined with a one-way ANOVA followed by Tukey's or Dunnett's multi comparison post hoc test. Statistical significance was set at $p < 0.05$.

Results

MLCK and myosin IIA are essential for *S. flexneri* cell-to-cell spreading in HeLa cells

Preliminary data from our laboratory suggested that HeLa cells infected with *Shigella* strains defective in cell-to-cell spreading (Δ*icsA* and R-LPS) strains have significantly reduced myosin IIA, but not IIB protein levels. Hence the study is focused on myosin IIA. ML-7 and ML-9 inhibit the catalytic activity of MLCK by out competing ATP binding, however ML-9 is more potent compared with ML-7 (Saitoh *et al.*, 1987). HeLa monolayers infected with *S. flexneri* were treated with increasing concentrations of ML-7 or ML-9 or with the DMSO vehicle alone (Fig. 1). ML-7 and ML-9 treatment reduced *Shigella* plaque size (Fig. 1A, C and E), but not plaque numbers (Fig. 1B and 1D). Treatment with 50 μM ML-9 abolished plaque formation altogether (Fig. 1D).

Blebbistatin exists in two (±) enantiomeric forms. The active (-) enantiomer (Straight *et al.*, 2003) preferentially binds the myosin II active site when ATP has been hydrolysed to the intermediate ADP and phosphate, hence slowing down phosphate release. Blebbistatin binding also locks myosin II in a state which reduces actin binding (Kovacs *et al.*, 2004; Ramamurthy *et al.*, 2004). HeLa monolayers infected with *S. flexneri* were treated with increasing concentrations of (+)-blebbistatin, (-)-blebbistatin or with the DMSO vehicle alone (Fig. 2A - C). Infectious foci formation was abolished when HeLa cells were treated with 50 μM (-)-blebbistatin (Fig. 2B). No effect on infectious foci formation was observed with the inactive (+)-enantiomer, as expected (Fig. 2A - C).

To examine the effect of myosin IIA depletion on *S. flexneri* cell-to-cell spreading, HeLa cells were transfected with myosin IIA (*MYH9*) siRNA and an infectious focus assay was carried out. Western immunoblots of HeLa cells lysates two days post siRNA treatment showed ~80% reduction in myosin IIA levels (Fig. 2D). *S. flexneri* formed infectious foci on HeLa cells treated with myosin IIA siRNA with a reduced mean focus area (***$p < 0.001$) (Fig. 2E and G) but not foci counts (Fig. 2F) when compared with HeLa cells treated with the negative control siRNA. Therefore myosin II inhibition with (-)-blebbistatin as well as myosin IIA siRNA knockdown reduced *Shigella* cell-to-cell spreading. Inhibition of MLCK with ML-7 and ML-9 also significantly reduced *Shigella* plaque formation.

MLCK and myosin II inhibitors do not affect bacterial replication and protrusion formation

The inability of *S. flexneri* to form plaques can be attributed to reduced bacterial replication or inability to mediate protrusion formation. Semi-confluent HeLa cells were initially infected with *S. flexneri* to allow bacterial invasion into HeLa cells before treatment with ML-7, ML-9 and (-)-blebbistatin. The number of intracellular bacteria was calculated at 1, 2, 4 and 6 h post incubation in gentamicin, which kills extracellular bacteria. As shown in Fig. 3A, HeLa cells treated with DMSO or MLCK or myosin II inhibitors had no adverse effect on the rate of intracellular replication.

Bacterial protrusion formation was also determined in HeLa cells treated with MLCK and myosin inhibitors. Semi-confluent HeLa cells were initially infected with *S. flexneri* to allow bacterial invasion into HeLa cells before treatment with ML-7, ML-9 and (-)-blebbistatin for 1.5 h. HeLa cells treated with DMSO or MLCK or myosin II inhibitors formed protrusions similar to untreated HeLa cells (Fig. 3C). No differences in % infected HeLa cells with bacterial protrusion were observed (Fig. 3B).

Myosin IIA is localised to the S. *flexneri* F-actin tail

The *S. flexneri* IcsA protein is localised at the old pole of the bacteria and interacts with the host N-WASP, which in turn recruits the Arp2/3 complex to initiate actin polymerisation. The F-actin tail that is formed imparts motility to the bacteria (Goldberg *et al.*, 1993; Suzuki *et al.*, 1998; Goldberg, 2001). The localisation of myosin IIA in *S. flexneri*-infected HeLa cells was investigated with IF microscopy. In untreated HeLa cells, myosin IIA is localised at the cytoplasm, cortex and stress fibers, and co-localises with the *S. flexneri* F-actin tail (Fig. 4A). This was similarly observed when HeLa cells were treated with DMSO and infected with *S. flexneri* (Fig. 4B). Treatment of infected HeLa cells with MLCK inhibitors, ML-7 and ML-9, did not affect myosin IIA localisation to bacterial F-actin tail (Fig. 4C and D).

HeLa cells were also treated with the myosin II inhibitor, blebbistatin. As expected treatment with the inactive (+) enantiomer did not affect myosin II localisation to the bacteria F-actin tail (Fig. 4E). Treatment with (-)-blebbistatin resulted in loss of stress fibres integrity and

exaggerated membrane ruffling (Fig. 4F). In myosin IIA siRNA-transfected cells, a reduction in cellular myosin IIA protein levels was observed, as expected (Fig 4G). Myosin II inhibition with (-)-blebbistatin and siRNA knockdown did not affect *S. flexneri* F-actin tail formation nor myosin IIA localisation to F-actin tail (Fig. 4F and G). The frequency of *S. flexneri* comet tail formation also did not differ between untreated cells, *MYH9* siRNA-transfected cells and cells treated with DMSO, ML-7, ML-9 or both enantiomers of blebbistatin (data not shown). Hence F-actin tail formation is not dependent on either MLCK or myosin IIA.

Two distinct myosin IIA staining patterns are observed in HeLa cells infected with *S. flexneri* R-LPS and Δ*icsA* strains

IcsA and LPS are important for *S. flexneri* cell-to-cell spreading. In R-LPS strains, IcsA polar localisation and ABM is affected, but bacteria can still invade cells (Sandlin *et al.*, 1995; Van Den Bosch *et al.*, 1997). R-LPS strains also form F-actin tails, albeit infrequently and are shortened and distorted (Van Den Bosch *et al.*, 1997). *S. flexneri* Δ*icsA* strains can invade cells but do not form F-actin tails and hence are defective in cell-to-cell spreading (Goldberg & Theriot, 1995; Van Den Bosch & Morona, 2003). The localisation of myosin IIA in HeLa cells infected with Δ*icsA* and R-LPS strains was investigated with IF microscopy. While myosin IIA was observed in infected HeLa cells, the level of staining observed varied greatly between WT *S. flexneri*, R-LPS, Δ*icsA* or Δ*icsA*, R-LPS-infected HeLa cells (Fig. 5A).

The relative myosin IIA fluorescence of infected HeLa cells was quantified by comparing myosin IIA staining intensity in infected HeLa cells relative to the mean staining intensity of two to three uninfected HeLa cells within the same image. The maximum intensity of uninfected HeLa cells was set at 100% (Fig. 5E). In HeLa cells infected with WT *S. flexneri* 2457T, myosin IIA staining did not differ from uninfected HeLa cells (90.59 ± 6.79 %) (Fig. 5A and E). HeLa cells infected with *S. flexneri* R-LPS (RMA723) had more intracellular bacteria in the cytoplasm (Fig. 5B - column 1) compared to the WT strain (Fig. 5A - column 1), presumably due to intercellular spreading defects. As seen in Fig. 5B (column 2), two different myosin IIA staining was observed. Infected HeLa cells either had similar myosin IIA protein levels compared to the WT 2475T infected-HeLa cells or had uniform loss of myosin IIA from the cytoplasm, cortex and stress fibers. These cells were marked with ‡. The myosin IIA fluorescence of the two

distinct cell populations [RMA723 and RMA723 (Lo - low myosin IIA protein levels)] was measured from 200 cells from two independent experiments and differed significantly (89.69 ± 3.97% vs 47.00 ± 1.43%, ***$p < 0.001$). The overall percentage of RMA723-infected cells with low myosin II protein levels was 25.30 ± 0.44% (Fig. 5F).

Significant bacterial clumping was observed in HeLa cells infected with *S. flexneri* Δ*icsA* strain (Fig. 5C - column 1) compared to HeLa cells infected with the R-LPS strain (Fig. 5B, column 1). Individual bacterium could not be distinguished due to the overcrowding of bacteria in the HeLa cell cytoplasm (Fig. 5C - column 1). This was expected since Δ*icsA* mutants are deficient in cell-to-cell spreading and are unable to spread laterally(delete). Similar to HeLa cells infected with the *S. flexneri* R-LPS strain, two distinct myosin IIA staining profiles were observed in HeLa cells infected with the Δ*icsA* strain (Fig. 5C - column 2). Infected HeLa cells with low myosin IIA staining were similarly marked with ‡ [RMA2041 (Lo)] and the mean myosin IIA intensity of this infected HeLa population was 54.43 ± 1.18%, which was significantly lower than RMA2041-infected HeLa cells with unaffected myosin IIA protein levels (91.36 ± 6.93%, **$p <$ 0.001). The overall percentage of RMA2041 (Δ*icsA*)-infected cells with low myosin II protein levels was 30.31 ± 0.72%, which was not significantly different from that of RMA723 (R-LPS)-infected cells (Fig. 5F).

HeLa cells were infected with *S. flexneri* Δ*icsA*, R-LPS double mutant (RMA2043) to investigate if there were any synergistic effect between the Δ*icsA* and R-LPS mutants (Fig. 5D). Similar to HeLa cells infected with the Δ*icsA* strain (Fig. 5C - column 1), individual bacterium could not be distinguished due to significant bacterial clumping in the HeLa cytosol (Fig. 5D - column 1). Two distinct myosin IIA staining profiles were also observed in RMA2043-infected HeLa cells (Fig. 5D - column 2), similar to the R-LPS and Δ*icsA* mutants (Fig. 5B and C, column 2). The difference in mean myosin IIA labelling intensity between RMA2043-infected HeLa cells with no loss of myosin IIA staining and infected HeLa cells with significant reduction in myosin IIA protein levels [RMA2043 (Lo)] was 82.27 ± 0.14% and 49.25 ± 0.14% (**$p < 0.001$), respectively. Hence, no further reduction in myosin IIA protein levels was observed when both IcsA and LPS were mutated. No differences in F-actin cytoskeletal staining were observed between infected HeLa cells with typical or reduced myosin IIA protein levels (Fig. 5D, column

3). The overall percentage of RMA2043 (Δ*icsA*, R-LPS)-infected cells with low myosin II protein levels was 43.97 ± 4.11%, which was higher (*$p < 0.05$) than RMA723 (R-LPS) and RMA2041 (Δ*icsA*)-infected cells (Fig. 5F). The increased frequency of infected HeLa cells with reduced myosin IIA staining in the double mutant suggests the mutations had a synergistic effect.

It is unclear how and why myosin IIA protein levels are decreased when infected with *S. flexneri* mutants defective in cell-to-cell spreading. The number of *S. flexneri* bacteria within the infected HeLa cell does not appear to be the distinguishing difference as bacterial loads appears to be similar between the two cell populations in either *S. flexneri* R-LPS, Δ*icsA* or Δ*icsA*, R-LPS-infected HeLa cells (Fig. 5B - D, column 1). Furthermore no changes to the cell shape or actin cytoskeleton is observed in spite of the reduced myosin IIA protein levels (Fig. 5B - D, column 3). The HeLa cell line used in this study also expresses myosin IIB (Betapudi, 2010). Myosin IIB localisation in HeLa cells during *S. flexneri* infection was investigated by IF microscopy (Fig. 6). Myosin IIB staining was similar to myosin IIA, but is more pronounced at the stress fibres. HeLa cells were infected with *S. flexneri* 2457T (WT), RMA723 (R-LPS), RMA2041 (Δ*icsA*) or RMA2043 (Δ*icsA*, R-LPS) and myosin IIB localisation was examined (Fig. 6). Similar levels of myosin IIB staining were observed in both infected and uninfected HeLa cells. It appears the distinctive myosin II staining in *S. flexneri* R-LPS or Δ*icsA*-infected HeLa cells is specific for isoform IIA.

Discussion

In an attempt to differentiate host proteins which are recruited to rough and smooth *Shigella* strains, we observed that myosin IIA but not IIB protein levels were significantly reduced in HeLa cells infected with R-LPS and Δ*icsA* strains. Previously inhibition of myosin II and its specific kinase, MLCK, reportedly reduced the size of *Shigella* foci of infection in Caco-2 cells (Rathman *et al.*, 2000). In a separate study, Mostowy *et al.* (2010) showed that in HeLa cells, myosin II was recruited to the septin cage which entraps intracytosolic *Shigella* without F-actin tails and targets the bacterium to the autophagy pathway for degradation. In this study the contribution of myosin IIA and MLCK during *Shigella* cell-to-cell spreading in HeLa cells was investigated with inhibitors and siRNA knockdown. The differences between myosin IIA and IIB labelling in *S. flexneri* R-LPS and Δ*icsA*-infected HeLa cells was also investigated.

382

383 *Shigella* intercellular spreading in host cells is dependent on its ability to initiate *de novo* F-actin
384 tail polymerisation, protrusion formation into neighbouring cells, engulfment of protrusions and
385 lysis of the double membrane vacuole, and is dependent on both *Shigella* and host proteins. In
386 eukaryotic cells, the cortical tension is maintain by the actin-myosin II (actomyosin) network
387 (Pasternak *et al.*, 1989) which is important for various processes such as lamellipodia formation
388 (Betapudi, 2010) and maintaining cell morphology (Eliott *et al.*, 1993; Wei & Adelstein, 2000;
389 Even-Ram *et al.*, 2007). Phosphorylation of myosin II regulatory light chain by a number of
390 kinases, including MLCK and Rho-activated kinase activate myosin II ATPase activity, filament
391 formation and contractile activity *in vitro* and *in vivo* (Conti *et al.*, 2008; Conti & Adelstein,
392 2008). Mammalian cells express three myosin II isoforms, IIA, IIB and IIC; however, in spite
393 high degree of similarity in sequence identity and structural conservation, myosin II isoforms
394 differ in enzymatic properties and subcellular localisation (Maupin *et al.*, 1994; Conti *et al.*,
395 2008). The isoforms also have distinct and redundant roles depending on the specific cellular
396 processes (Kelley *et al.*, 1996; Kolega, 1998; Betapudi, 2010; Wang *et al.*, 2011).
397

398 Inhibition of MLCK and myosin II catalytic activity with ML-7, ML-9 and (-)-blebbistatin
399 significantly reduced *Shigella* intercellular spreading. Knockdown of myosin IIA with siRNA
400 similarly affected *Shigella* cell-to-cell spreading. Myosin IIA knockdown was not complete as
401 low levels of the protein was detected with Western immunoblotting. Nonetheless myosin IIA
402 inhibition reduced *Shigella* infectious focus area by > 60%. These results also suggest myosin
403 IIB is unable to rescue myosin IIA function and that myosin IIA's role in *Shigella* cell-to-cell
404 spreading is specific. These results are in agreement with previous findings that showed MLCK
405 involvement during *Shigella* intercellular spreading in polarised Caco-2 cells (Rathman *et al.*,
406 2000). The authors also provided indirect evident for myosin II involvement (Rathman *et al.*,
407 2000).
408

409 The inability to form plaques or infectious foci could be attributed to either reduced bacterial
410 motility or lack of protrusion formation. *Shigella* F-actin tail formation occurred at a similar
411 frequency to untreated cells. Furthermore *Shigella* protrusion formation in semi-confluent HeLa
412 cells was also not significantly affected. This was in contrast to the previous report in confluent

Caco-2 cells where ML-7 inhibited *Shigella* protrusion formation as detected by transmission electron microscopy. In the few protrusions that were observed, *Shigella* bacteria was not tightly associated with the protruding membrane (Rathman *et al.*, 2000). While that study primarily used Caco-2 cells, the authors also used semi-confluent HeLa cells to observe F-actin tail formation in the presence of ML-7. Both *Shigella* F-actin tail and protrusion formation were observed and were not significantly different from untreated, infected HeLa cells in that study, as we also observed (Rathman *et al.*, 2000). No differences in *Shigella* viable cell counts were observed for ML-7, ML-9 and (-)-blebbistatin-treated HeLa cells, suggesting *Shigella* growth is unaffected. Hence the most likely explanation for reduced *Shigella* plaque or foci formation in the absence of MLCK and myosin II is likely due to a defect in the uptake of bacteria-containing protrusion into the neighbouring cells.

In Mostowy *et al.* (2010)'s study, myosin II depletion with siRNA increased the number of *Shigella*-infected cells 4 h 40 min post-infection when observed with quantitative microscopy. Similar results were observed by flow cytometry when Caco-2 cells were treated with the myosin II inhibitor, blebbistatin (Mostowy *et al.*, 2010). To rule out the possibility that myosin II inactivation increased *Shigella* cell-to-cell spread independently of septin caging, blebbistatin treatment was repeated with *Listeria monocytogenes*-infected Caco-2 cells (Mostowy *et al.*, 2010). *Listeria* also relies on F-actin tail formation for cell-to-cell spread (Gouin *et al.*, 2005), but septin caging was not observed under similar experimental conditions (Mostowy *et al.*, 2010). Blebbistatin treatment did not increase, and even slightly reduced the number of *Listeria*-infected Caco-2 cells and it was inferred loss of myosin II does not affect *Shigella* cell-to-cell spread and that inactivation of septin caging alone was responsible for the increase in *Shigella* intercellular spreading.

The conclusion in reference to the role of myosin II and *Shigella* cell-to-cell spreading from Mostowy *et al.* (2010)'s study would appear contradictory to our findings and that of Rathman *et al.* (2000). The main issue with using *Listeria* as an alternative model is that myosin II and MLCK are not required for *Listeria* cell-to-cell spread regardless of septin caging. This has been demonstrated by various groups in *Potorous tridactylis* kidney (PtK2) cells (Cramer & Mitchison, 1995), Caco-2 cells (Rathman *et al.*, 2000) and Caco-2 BBE1 cells (Rajabian *et al.*,

2009). Hence the role of myosin II in *Shigella* intercellular spreading during septin caging of non-motile *Shigella*-infected HeLa cells requires further investigation. It is likely myosin II plays different roles during different stages of *Shigella* infection. Myosin II interaction with septin initially helps to target a subset of non-motile *Shigella* for destruction via autophagy. *Shigella* bacteria which have successfully initiated F-actin tail undergo replication and subsequently form protrusions into the neighbouring cells, whereby myosin II facilitates uptake of the bacterium. Depending on the experimental conditions, myosin II inhibition would result in different outcomes. In Mostowy *et al.* (2010)'s study, the number of infected cells were determined out 4 h 40 min post infection whereas plaque and infectious focus formation are typically measured 24 - 48 h post infection.

The *Shigella* IcsA outer membrane protein is localised to the old pole, ie the pole which exists prior to cellular division which gives rise to new daughter poles (Goldberg *et al.*, 1993). IcsA polar localisation is also dependent on LPS. Shortening of LPS O-antigen chain length has revealed IcsA expression on the lateral surface of *Shigella* (Morona & Van Den Bosch, 2003). Hence LPS may act to mask IcsA on the lateral regions to reinforce polar localisation. Alterations of LPS O-antigen chain length also affect ABM and *Shigella* plaque formation adversely (Morona *et al.*, 2003). In infected HeLa cells, myosin IIA and IIB were found at *Shigella* F-actin tail. However only myosin IIA protein levels in HeLa cells were significantly reduced (~50%) when infected with *Shigella* Δ*icsA* and R-LPS strains. This was observed in ~25 - 30% of infected cells. No further decrease in myosin IIA labelling was observed when cells were infected with the Δ*icsA*, R-LPS double mutant, although the proportion of cells with reduced myosin IIA was almost doubled. This suggests that there might be some synergistic effects between Δ*icsA* and R-LPS mutations, although it is unclear how this interaction may occur. *Shigella* Δ*icsA* and R-LPS strains are defective in cell-to-cell spreading and over time, bacterial clumps accumulate within the HeLa cell cytoplasm. The uniform loss of myosin IIA could be partly attributed to the increased bacterial loads in HeLa cells. However infected cells with similar bacterial numbers can have either similar or decreased myosin IIA protein levels compared to uninfected neighbouring HeLa cells (Fig. 5). Nonetheless the increased bacterial load in the cytoplasm may trigger activation of an undefined signalling pathway which in turn decreases myosin IIA levels.

In addition to its role in *Shigella* cell-to-cell spreading, recent studies implicate myosin II in the pathogenesis of several important bacterial pathogens such as *Chlamydia, Salmonella Helicobacter*. In *Chlamydia*, myosin IIA and IIB are required for extrusion egress following chlamydial development within a vacuole in the host. In the absence of myosin IIA and IIB activation, lytic egress is favoured (Lutter *et al.*, 2013). The balance between lytic and extrusion egress mechanism is achieved in response to cellular signalling pathways and external environmental stimuli (Lutter *et al.*, 2013). In *Salmonella*, the bacterial SopB protein mediates myosin IIA-dependent contractility, forming stress-fibre like structures which is thought to facilitate *Salmonella* entry into the host cell (Hänisch *et al.*, 2011). Additionally myosin IIB induces cytoskeletal rearrangements around the *Salmonella*-containing vacuole (SCV) in the host cell, which may act to restrain bacterial growth and regulate bacterial virulence (Odendall *et al.*, 2012). Myosin IIA has also been reported to facilitate positioning of the SCV at the host nucleus (Wasylnka *et al.*, 2008). In *Helicobacter*, increased myosin II activity resulted in subsequent loss of gastric mucosal tight junction barrier integrity which may contribute to the predisposition of gastric cancer development of (remove) (Posselt *et al.*, 2013). In non-polarised gastric epithelial cells, inhibition of myosin II activity affected the rear retraction of the cell resulting in significantly altered cell shape (Lu *et al.*, 2009), which may contribute to gastric carcinoma invasion and metastasis (Argent *et al.*, 2004; Azuma *et al.*, 2004; Basso *et al.*, 2008). Hence myosin IIA and IIB play diverse roles during pathogenesis of different intracellular pathogens, which is distinct from its role in *Shigella* intercellular spread. In some cases, only one of the myosin II isoform is required suggesting myosin II specificity.

Although we initially set out to identify host proteins which are differentially localised to *Shigella* smooth and rough strains, it was unexpectedly observed that *Shigella* strains defective in cell-to-cell spreading had reduced myosin IIA, but not IIB protein levels in a proportion of infected HeLa cells, suggesting specificity between the two isoforms. This was not surprising since myosin II isoforms have been reported to play different roles within the same cell type (Maupin *et al.*, 1994; Betapudi, 2010). Furthermore different myosin II isoforms are also targeted by bacteria at different stages of infection, as in the case of *Salmonella*.

We also show that MLCK and myosin IIA inhibition significantly affected *Shigella* plaque formation but no effect on intracellular growth and protrusion formation was observed. Low levels of myosin IIA was detected in the *Shigella* F-actin tails. We hypothesize that the reduced plaque formation could be a defect in the uptake of bacteria-containing protrusion in the neighbouring cells. Previously components of the clathrin mediated endocytic pathway including dynamin, clathrin and Epsin-1 was shown to mediate bacterial uptake in the neighbouring cells (Fukumatsu *et al.*, 2012; Lum *et al.*, 2013). It is possible myosin IIA may interact with components of the endocytic pathway to facilitate uptake of bacteria-containing protrusions. Perhaps the loss of *icsA* or LPS O-antigen affected *Shigella* cell-to-cell spreading which led to downstream effects including bacterial overcrowding of HeLa cell cytoplasm, which in turn affected myosin IIA expression.

Acknowledgements

We thank Luisa Van Den Bosch for preliminary work on myosin IIA. This work is supported by a Program Grant (565526) from the National Health and Medical Research Council (NHMRC) of Australia. ML was the recipient of the Australian Postgraduate Award from the NHMRC. The authors declare that they have no conflict of interest.

References

Argent RH, Kidd M, Owen RJ, Thomas RJ, Limb MC & Atherton JC (2004) Determinants and consequences of different levels of CagA phosphorylation for clinical isolates of *Helicobacter pylori*. *Gastroenterology* **127**: 514-523.

Azuma T, Yamazaki S, Yamakawa A *et al.* (2004) Association between diversity in the Src homology 2 domain--containing tyrosine phosphatase binding site of *Helicobacter pylori* CagA protein and gastric atrophy and cancer. *J Infect Dis* **189**: 820-827.

Basso D, Zambon CF, Letley DP *et al.* (2008) Clinical relevance of *Helicobacter pylori cagA* and *vacA* gene polymorphisms. *Gastroenterology* **135**: 91-99.

Bernardini ML, Mounier J, d'Hauteville H, Coquis-Rondon M & Sansonetti PJ (1989) Identification of *icsA*, a plasmid locus of *Shigella flexneri* that governs bacterial intra- and intercellular spread through interaction with F-actin. *Proc Natl Acad Sci U S A* **86**: 3867-3871.

Betapudi V (2010) Myosin II motor proteins with different functions determine the fate of lamellipodia extension during cell spreading. *PLoS One* **5**: e8560.

Bishai EA, Sidhu GS, Li W, Dhillon J, Bohil AB, Cheney RE, Hartwig JH & Southwick FS (2012) Myosin-X facilitates *Shigella*-induced membrane protrusions and cell-to-cell spread. *Cell Microbiol* **15**: 353–367.

Conti M, Kawamoto S & Adelstein R (2008) Nonmuscle myosin II. *Myosins: A Superfamily of Molecular Motors,* Vol. 7 (Coluccio L, ed), pp. 223-264. Springer, Dordrecht.

Conti MA & Adelstein RS (2008) Nonmuscle myosin II moves in new directions. *J Cell Sci* **121**: 11-18.

Cossart P & Sansonetti PJ (2004) Bacterial invasion: The paradigms of enteroinvasive pathogens. *Science* **304**: 242-248.
Cramer LP & Mitchison TJ (1995) Myosin is involved in postmitotic cell spreading. *J Cell Biol* **131**: 179-189.
Eliott S, Joss GH, Spudich A & Williams KL (1993) Patterns in *Dictyostelium discoideum*: the role of myosin II in the transition from the unicellular to the multicellular phase. *J Cell Sci* **104**: 457-466.
Esue O, Harris ES, Higgs HN & Wirtz D (2008) The filamentous actin cross-linking/bundling activity of mammalian formins. *J Mol Biol* **384**: 324-334.
Even-Ram S, Doyle AD, Conti MA, Matsumoto K, Adelstein RS & Yamada KM (2007) Myosin IIA regulates cell motility and actomyosin-microtubule crosstalk. *Nat Cell Biol* **9**: 299-309.
Fukumatsu M, Ogawa M, Arakawa S, Suzuki M, Nakayama K, Shimizu S, Kim M, Mimuro H & Sasakawa C (2012) *Shigella* targets epithelial tricellular junctions and uses a noncanonical clathrin-dependent endocytic pathway to spread between cells. *Cell Host Microbe* **11**: 325-336.
Goldberg MB (2001) Actin-based motility of intracellular microbial pathogens. *Microbiol Mol Biol Rev* **65**: 595-626.
Goldberg MB & Theriot JA (1995) *Shigella flexneri* surface protein IcsA is sufficient to direct actin-based motility. *Proc Natl Acad Sci U S A* **92**: 6572-6576.
Goldberg MB, Barzu O, Parsot C & Sansonetti PJ (1993) Unipolar localization and ATPase activity of IcsA, a *Shigella flexneri* protein involved in intracellular movement. *J. Bacteriol.* **175**: 2189-2196.
Gouin E, Welch MD & Cossart P (2005) Actin-based motility of intracellular pathogens. *Current Opinion in Microbiology* **8**: 35-45.
Hänisch J, Kölm R, Wozniczka M, Bumann D, Rottner K & Stradal Theresia EB (2011) Activation of a RhoA/Myosin II-dependent but Arp2/3 complex-independent pathway facilitates *Salmonella* invasion. *Cell Host & Microbe* **9**: 273-285.
Heindl JE, Saran I, Yi C-r, Lesser CF & Goldberg MB (2009) Requirement for formin-induced actin polymerization during spread of *Shigella*. *Infect Immun* **78**: 193-203.
Hong M & Payne SM (1997) Effect of mutations in *Shigella flexneri* chromosomal and plasmid-encoded lipopolysaccharide genes on invasion and serum resistance. *Mol Microbiol* **24**: 779-791.
Kadurugamuwa JL, Rohde M, Wehland J & Timmis KN (1991) Intercellular spread of *Shigella flexneri* through a monolayer mediated by membranous protrusions and associated with reorganization of the cytoskeletal protein vinculin. *Infect Immun* **59**: 3463-3471.
Kelley CA, Sellers JR, Gard DL, Bui D, Adelstein RS & Baines IC (1996) *Xenopus* nonmuscle myosin heavy chain isoforms have different subcellular localizations and enzymatic activities. *J Cell Biol* **134**: 675-687.
Kolega J (1998) Cytoplasmic dynamics of myosin IIA and IIB: spatial 'sorting' of isoforms in locomoting cells. *J Cell Sci* **111**: 2085-2095.
Kotloff KL, Noriega F, Losonsky GA, Sztein MB, Wasserman SS, Nataro JP & Levine MM (1996) Safety, immunogenicity, and transmissibility in humans of CVD 1203, a live oral *Shigella flexneri* 2a vaccine candidate attenuated by deletions in *aroA* and *virG*. *Infect Immun* **64**: 4542-4548.
Kovacs M, Toth J, Hetenyi C, Malnasi-Csizmadia A & Sellers JR (2004) Mechanism of blebbistatin inhibition of myosin II. *J Biol Chem* **279**: 35557-35563.
Lett MC, Sasakawa C, Okada N, Sakai T, Makino S, Yamada M, Komatsu K & Yoshikawa M (1989) *virG,* a plasmid-coded virulence gene of *Shigella flexneri*: identification of the *virG* protein and determination of the complete coding sequence. *J Bacteriol* **171**: 353-359.
Lu H, Murata-Kamiya N, Saito Y & Hatakeyama M (2009) Role of partitioning-defective 1/microtubule affinity-regulating kinases in the morphogenetic activity of *Helicobacter pylori* CagA. *J Biol Chem* **284**: 23024-23036.

Lum M, Attridge SR & Morona R (2013) Impact of dynasore an inhibitor of dynamin II on *Shigella flexneri* infection. *PLoS ONE* **8**: e84975.
Lutter Erika I, Barger Alexandra C, Nair V & Hackstadt T (2013) *Chlamydia trachomatis* inclusion membrane protein CT228 recruits elements of the myosin phosphatase pathway to regulate release mechanisms. *Cell Reports* **3**: 1921-1931.
Makino S, Sasakawa C, Kamata K, Kurata T & Yoshikawa M (1986) A genetic determinant required for continuous reinfection of adjacent cells on large plasmid in *S. flexneri* 2a. *Cell* **46**: 551-555.
Maupin P, Phillips CL, Adelstein RS & Pollard TD (1994) Differential localization of myosin-II isozymes in human cultured cells and blood cells. *J Cell Sci* **107**: 3077-3090.
Miyoshi J & Takai Y (2005) Molecular perspective on tight-junction assembly and epithelial polarity. *Adv Drug Deliv Rev* **57**: 815-855.
Morona R & Van Den Bosch L (2003) Lipopolysaccharide O antigen chains mask IcsA (VirG) in *Shigella flexneri*. *FEMS Microbiol Lett* **221**: 173-180.
Morona R, Daniels C & Van Den Bosch L (2003) Genetic modulation of *Shigella flexneri* 2a lipopolysaccharide O antigen modal chain length reveals that it has been optimized for virulence. *Microbiol.* **149**: 925-939.
Mostowy S, Bonazzi M, Hamon MA *et al.* (2010) Entrapment of intracytosolic bacteria by septin cage-like structures. *Cell Host & Microbe* **8**: 433-444.
Oaks EV, Wingfield ME & Formal SB (1985) Plaque formation by virulent *Shigella flexneri*. *Infect Immun* **48**: 124-129.
Odendall C, Rolhion N, Förster A, Poh J, Lamont Douglas J, Liu M, Freemont Paul S, Catling Andrew D & Holden David W (2012) The *Salmonella* Kinase SteC targets the MAP kinase MEK to regulate the host actin cytoskeleton. *Cell Host & Microbe* **12**: 657-668.
Okamura N, Nagai T, Nakaya R, Kondo S, Murakami M & Hisatsune K (1983) HeLa cell invasiveness and O antigen of *Shigella flexneri* as separate and prerequisite attributes of virulence to evoke keratoconjunctivitis in guinea pigs. *Infect. Immun.* **39**: 505-513.
Pasternak C, Spudich JA & Elson EL (1989) Capping of surface receptors and concomitant cortical tension are generated by conventional myosin. *Nature* **341**: 549-551.
Posselt G, Backert S & Wessler S (2013) The functional interplay of *Helicobacter pylori* factors with gastric epithelial cells induces a multi-step process in pathogenesis. *Cell Commun Signal* **11**: 77.
Rajabian T, Gavicherla B, Heisig M, Muller-Altrock S, Goebel W, Gray-Owen SD & Ireton K (2009) The bacterial virulence factor InlC perturbs apical cell junctions and promotes cell-to-cell spread of *Listeria*. *Nat Cell Biol* **11**: 1212-1218.
Ramamurthy B, Yengo CM, Straight AF, Mitchison TJ & Sweeney HL (2004) Kinetic mechanism of blebbistatin inhibition of nonmuscle myosin IIb. *Biochemistry* **43**: 14832-14839.
Rathman M, de Lanerolle P, Ohayon H, Gounon P & Sansonetti P (2000) Myosin light chain kinase plays an essential role in *S. flexneri* dissemination. *J Cell Sci* **113**: 3375-3386.
Rohatgi R, Ma L, Miki H, Lopez M, Kirchhausen T, Takenawa T & Kirschner MW (1999) The interaction between N-WASP and the Arp2/3 complex links Cdc42-dependent signals to actin assembly. *Cell* **97**: 221-231.
Saitoh M, Ishikawa T, Matsushima S, Naka M & Hidaka H (1987) Selective inhibition of catalytic activity of smooth muscle myosin light chain kinase. *J Biol Chem* **262**: 7796-7801.
Sandlin RC, Lampel KA, Keasler SP, Goldberg MB, Stolzer AL & Maurelli AT (1995) Avirulence of rough mutants of *Shigella flexneri*: requirement of O antigen for correct unipolar localization of IcsA in the bacterial outer membrane. *Infect Immun* **63**: 229-237.
Sansonetti PJ, Mounier J, Prévost MC & Mege RM (1994) Cadherin expression is required for the spread of *Shigella flexneri* between epithelial cells. *Cell* **76**: 829-839.

Sansonetti PJ, Ryter A, Clerc P, Maurelli AT & Mounier J (1986) Multiplication of *Shigella flexneri* within HeLa cells: lysis of the phagocytic vacuole and plasmid-mediated contact hemolysis. *Infect Immun* **51**: 461-469.

Sansonetti PJ, Arondel J, Huerre M, Harada A & Matsushima K (1999) Interleukin-8 controls bacterial transepithelial translocation at the cost of epithelial destruction in experimental shigellosis. *Infect Immun* **67**: 1471-1480.

Sansonetti PJ, Phalipon A, Arondel J, Thirumalai K, Banerjee S, Akira S, Takeda K & Zychlinsky A (2000) Caspase-1 activation of IL-1β and IL-18 are essential for *Shigella flexneri*-induced inflammation. *Immunity* **12**: 581-590.

Schuch R, Sandlin RC & Maurelli AT (1999) A system for identifying post-invasion functions of invasion genes: requirements for the Mxi-Spa type III secretion pathway of *Shigella flexneri* in intercellular dissemination. *Mol Microbiol* **34**: 675-689.

Senerovic L, Tsunoda SP, Goosmann C, Brinkmann V, Zychlinsky A, Meissner F & Kolbe M (2012) Spontaneous formation of IpaB ion channels in host cell membranes reveals how *Shigella* induces pyroptosis in macrophages. *Cell Death Dis* **3**: e384.

Straight AF, Cheung A, Limouze J, Chen I, Westwood NJ, Sellers JR & Mitchison TJ (2003) Dissecting temporal and spatial control of cytokinesis with a myosin II Inhibitor. *Science* **299**: 1743-1747.

Suzuki T, Miki H, Takenawa T & Sasakawa C (1998) Neural Wiskott-Aldrich syndrome protein is implicated in the actin-based motility of *Shigella flexneri*. *EMBO J* **17**: 2767-2776.

Tran Van Nhieu G, Clair C, Bruzzone R, Mesnil M, Sansonetti P & Combettes L (2003) Connexin-dependent inter-cellular communication increases invasion and dissemination of *Shigella* in epithelial cells. *Nat Cell Biol* **5**: 720-726.

Van Den Bosch L & Morona R (2003) The actin-based motility defect of a *Shigella flexneri rmlD* rough LPS mutant is not due to loss of IcsA polarity. *Microb Pathog* **35**: 11-18.

Van Den Bosch L, Manning PA & Morona R (1997) Regulation of O-antigen chain length is required for *Shigella flexneri* virulence. *Mol Microbiol* **23**: 765-775.

Wang A, Ma X, Conti MA & Adelstein RS (2011) Distinct and redundant roles of the non-muscle myosin II isoforms and functional domains. *Biochem Soc Trans* **39**: 1131-1135.

Wasylnka JA, Bakowski MA, Szeto J, Ohlson MB, Trimble WS, Miller SI & Brumell JH (2008) Role for Myosin II in regulating positioning of *Salmonella*-containing vacuoles and intracellular replication. *Infection and Immunity* **76**: 2722-2735.

Wei Q & Adelstein RS (2000) Conditional expression of a truncated fragment of nonmuscle myosin II-A alters cell shape but not cytokinesis in HeLa cells. *Mol Biol Cell* **11**: 3617-3627.

Zychlinsky A, Prévost MC & Sansonetti PJ (1992) *Shigella flexneri* induces apoptosis in infected macrophages. *Nature* **358**: 167-169.

673 **Table 1. Bacterial strains**

Strain	Relevant characteristics[#]	Reference or source
S. flexneri		
2457T	*S. flexneri* 2a wild type	Laboratory collection
MLRM107	2457T [pMP7604; Tc^R]	(Lum *et al.*, 2013)
RMA723	2457T *ΔrmlD*::Km^R	(Van Den Bosch *et al.*, 1997)
RMA2041	2457T *ΔicsA*::Tc^R	(Van Den Bosch & Morona, 2003)
RMA2043	RMA2041 *ΔrmlD*::Km^R	(Van Den Bosch & Morona, 2003)

674 # Tc^R, Tetracycline resistant; Km^R, Kanamycin resistant

675

Figures

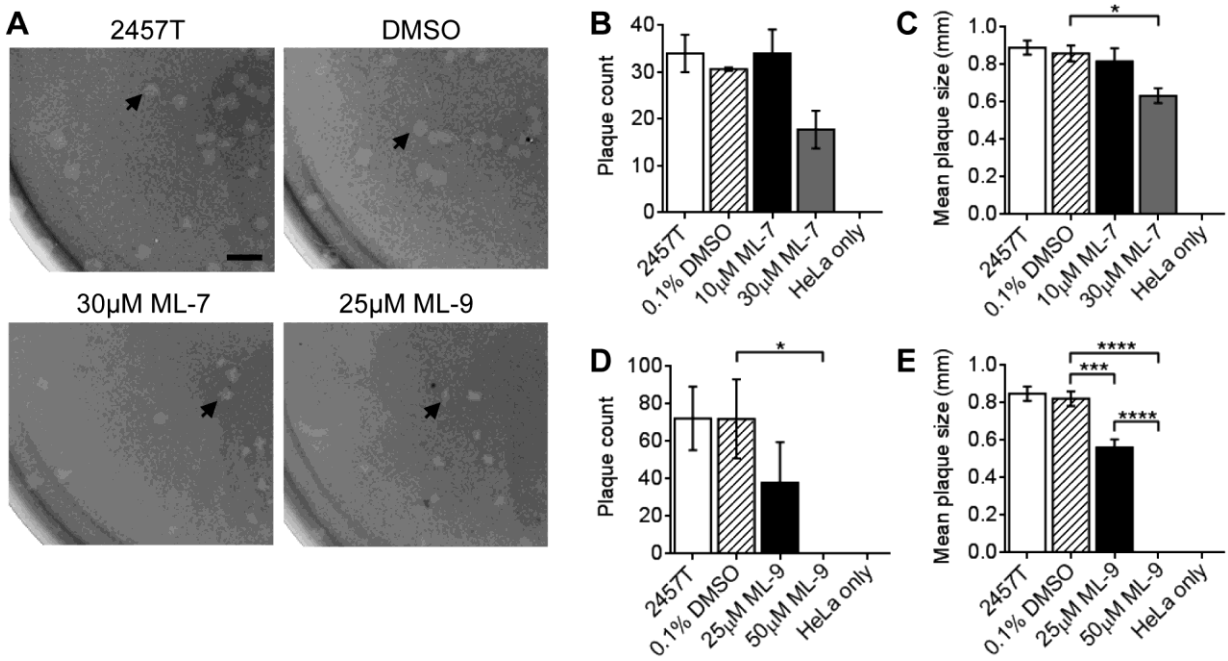

Fig. 1 MLCK inhibition reduces *S. flexneri* 2457T plaque size. HeLa cells were infected with *S. flexneri* 2457T in a plaque assay using a 6-well tray as described in the Methods. Plaque formation was performed in the presence of increasing concentrations of ML-7, ML-9 or the vehicle, 0.1 % DMSO. (A) Wells were stained with Neutral Red to makes plaques more visible. Scale bar = 2 mm. (B) The total plaque counts or (C) mean plaque diameters from each well treated with ML-7 and infected with *Shigella* were calculated. (D) The total plaque counts or (E) mean plaque diameters from each well treated with ML-9 and infected with *Shigella* were calculated. Data are represented as mean ± SEM of independent experiments (n = 3), analysed with one-way ANOVA ($p < 0.0001$ for ML-7 plaque counts and mean plaque diameters, $p = 0.0029$ for ML-9 plaque counts and $p < 0.0001$ for ML-9 plaque size), followed by Tukey's post hoc test (*$p < 0.05$, ***$p < 0.001$, ****$p < 0.0001$).

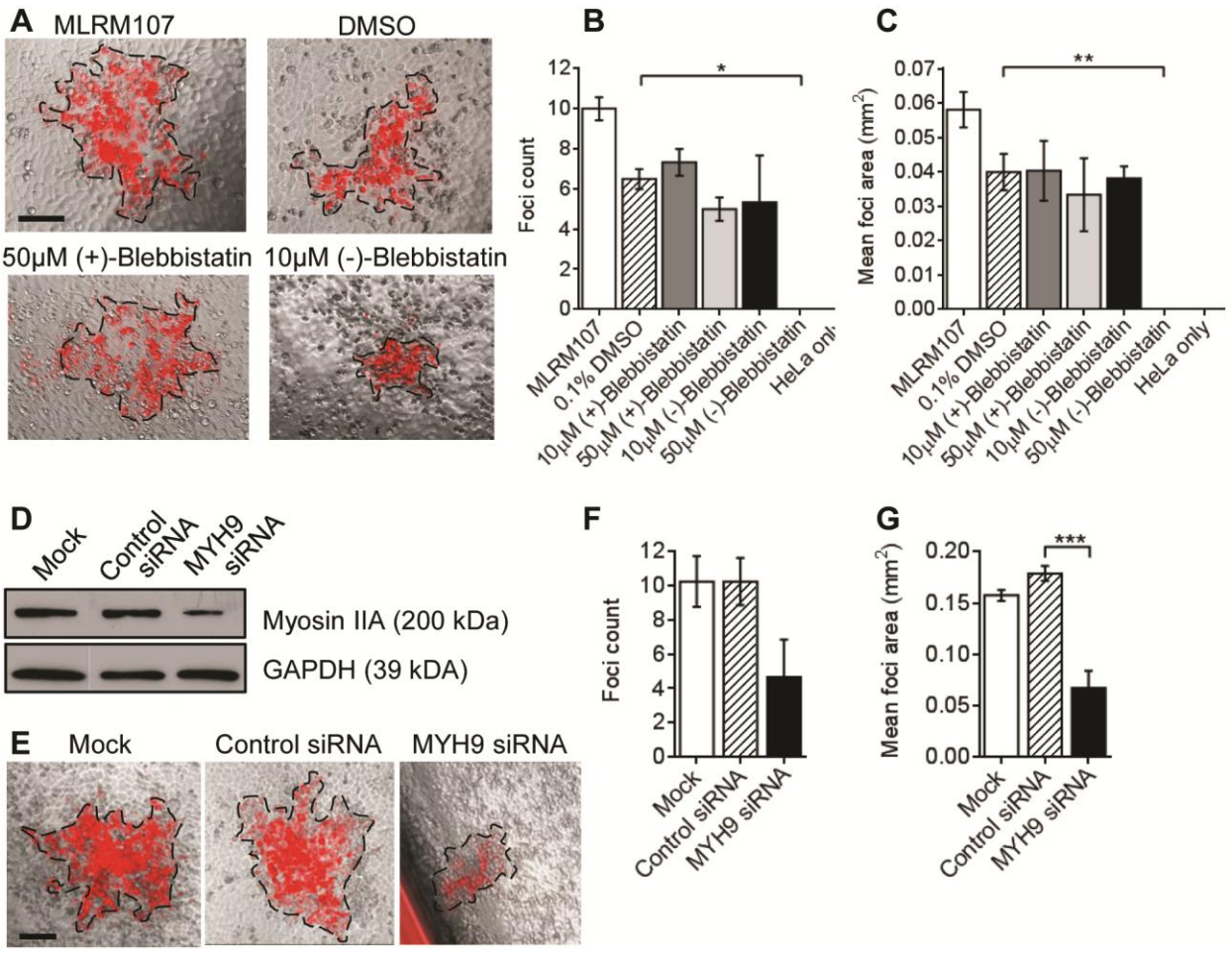

Fig. 2 Myosin IIA inhibition with (-)-blebbistatin and transfection of HeLa cells with *MYH9* siRNA reduces MLRM107 foci area. (A) - (C) HeLa cells were infected with *S. flexneri* MLRM107 in an infectious focus assay using a 12-well tray as described in the Methods. Infectious foci were imaged 24 h post gentamicin treatment. ≥ 15 infectious foci were imaged for each condition. (A) Images shown are overlay of an image taken with phase contrast and TxRed filter (10× magnification). The area of the infection focus i.e. area where mCherry was expressed, is outlined. Scale bar = 0.1 mm. (B) The total foci counts from one well or (C) mean foci area from one well were calculated. Data are represented as mean ± SEM of independent experiments (n = 3), analysed with one-way ANOVA ($p < 0.0001$ for foci counts and mean foci area), followed by Tukey's post hoc test (*$p < 0.05$, **$p < 0.01$). (D) - (G) HeLa cells were either mock transfected or transfected with control or *MYH9* (myosin IIA) siRNA for 24 h, trypsinised and re-transfected for further 24 h. (D) HeLa cell extracts were probed with anti-Myosin IIA. GAPDH was used as a loading control. (E - G) Post transfection, HeLa cells were infected and

infectious foci were imaged as described in (A) - (C). (E) Images shown are overlay of an image taken with phase contrast and TxRed filter (10× magnification). The area of the infection focus i.e. area where mCherry was expressed, is outlined. Scale bar = 0.1 mm. (F) The total foci counts from one well or (G) mean foci area from one well were calculated. Data are represented as mean ± SEM of independent experiments (n = 3), analysed with one-way ANOVA ($p > 0.05$ for foci counts and $p = 0.0003$ mean foci area), followed by Tukey's post hoc test (***$p < 0.001$).

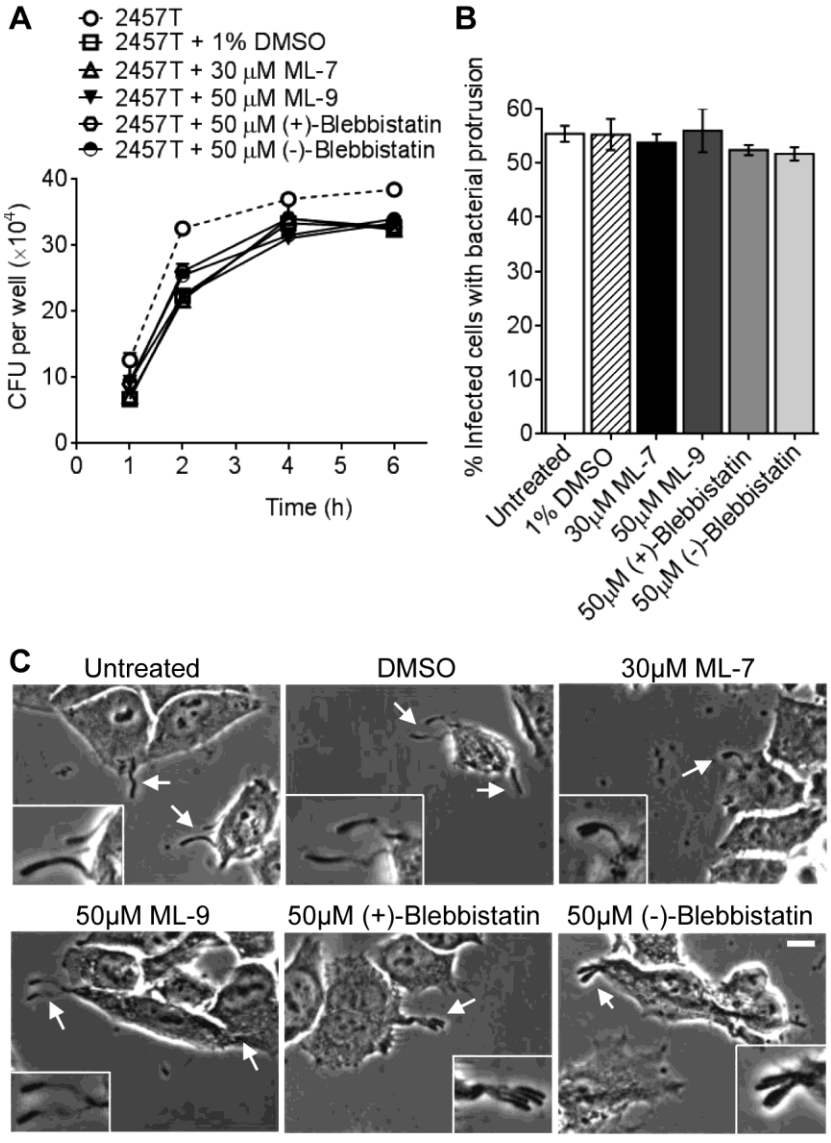

Fig. 3 *S. flexneri* 2457T intracellular growth and protrusion formation in HeLa cells are not affected by of ML-7, ML-9, (+)-blebbistatin and (-)-blebbistatin. HeLa cells were infected with *S. flexneri* 2457T for 1 h in a 24-well tray. HeLa cells were washed thrice with D-PBS and incubated with MEM containing 40 μg mL^{-1} of gentamicin (t = 0) to exclude extracellular bacteria. Concurrently HeLa cells were treated with 30 μM ML-7, 50 μM ML-9, 50 μM (+)-blebbistatin, 50 μM (-)-blebbistatin or DMSO. (A) To determine bacterial intracellular growth, two wells were prepared for each time point (t = 1, 2, 4 and 6 h) for each condition. At each interval, HeLa cells were washed, followed by lysis with 0.1% Triton X-100 to recover intracellular bacteria. Data are represented as mean from two-three independent experiments. (B

- C) At t = 1.5, HeLa cells were fixed to observe bacteria protrusions. (B) The percentage of infected cells with bacteria protrusion(s) were enumerated by counting >100 cells in each independent experiment. Data are represented as mean ± SEM of independent experiments (n = 2), analysed with one-way ANOVA ($p > 0.05$). (C) Infected HeLa cells were imaged at 40× magnification. Scale bar = 10 μm. The arrows indicate protrusion formation. Insert shows 2× enlargement of the indicated region.

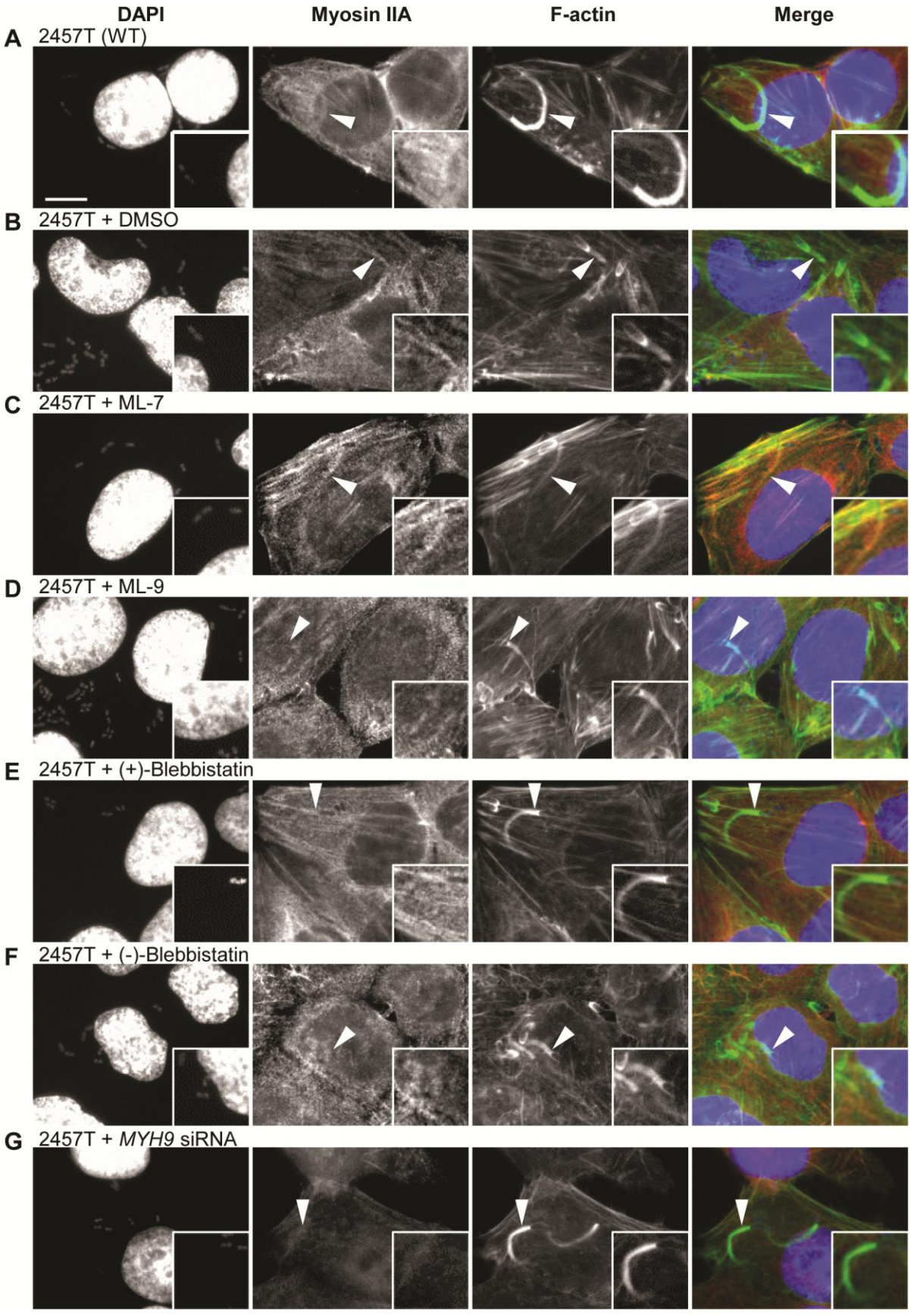
DAPI
Myosin IIA
F-actin
Merge
A
2457T (WT)
B
2457T + DMSO
C
2457T + ML-7
D
2457T + ML-9
E
2457T + (+)-Blebbistatin
F
2457T + (-)-Blebbistatin
G
2457T + MYH9 siRNA

Fig. 4 Myosin IIA is localised to the *S. flexneri* 2457T F-actin tail and is not affected by MLCK and myosin II inhibitors. HeLa cells were infected with *S. flexneri* 2457T in an invasion assay as described in the Methods. Bacteria and HeLa nuclei were stained with DAPI (blue), F-actin was stained with FITC-phalloidin (green) and myosin IIA was stained with anti-myosin IIA and Alexa Fluor 594-conjugated secondary antibody (red). Images were taken at 100× magnification. Scale bar = 10 μm. HeLa cells were treated with DMSO, ML-7, ML-9, (+)-blebbistatin, (-)-blebbistatin or were transfected with *MYH9* siRNA and were infected with *S. flexneri* 2457T; (A) Untreated; (B) 1% DMSO; (C) 30 μM ML-7; (D) 50 μM ML-9; (E) 50 μM (+)-blebbistatin; (F) 50 μM (-)-blebbistatin; (G) *MYH9* siRNA-transfected HeLa cells. Arrowheads indicate myosin IIA localisation at F-actin comet tails. Insert shows 1.5× enlargement of the indicated region. The experiment was repeated twice and representative images are shown.

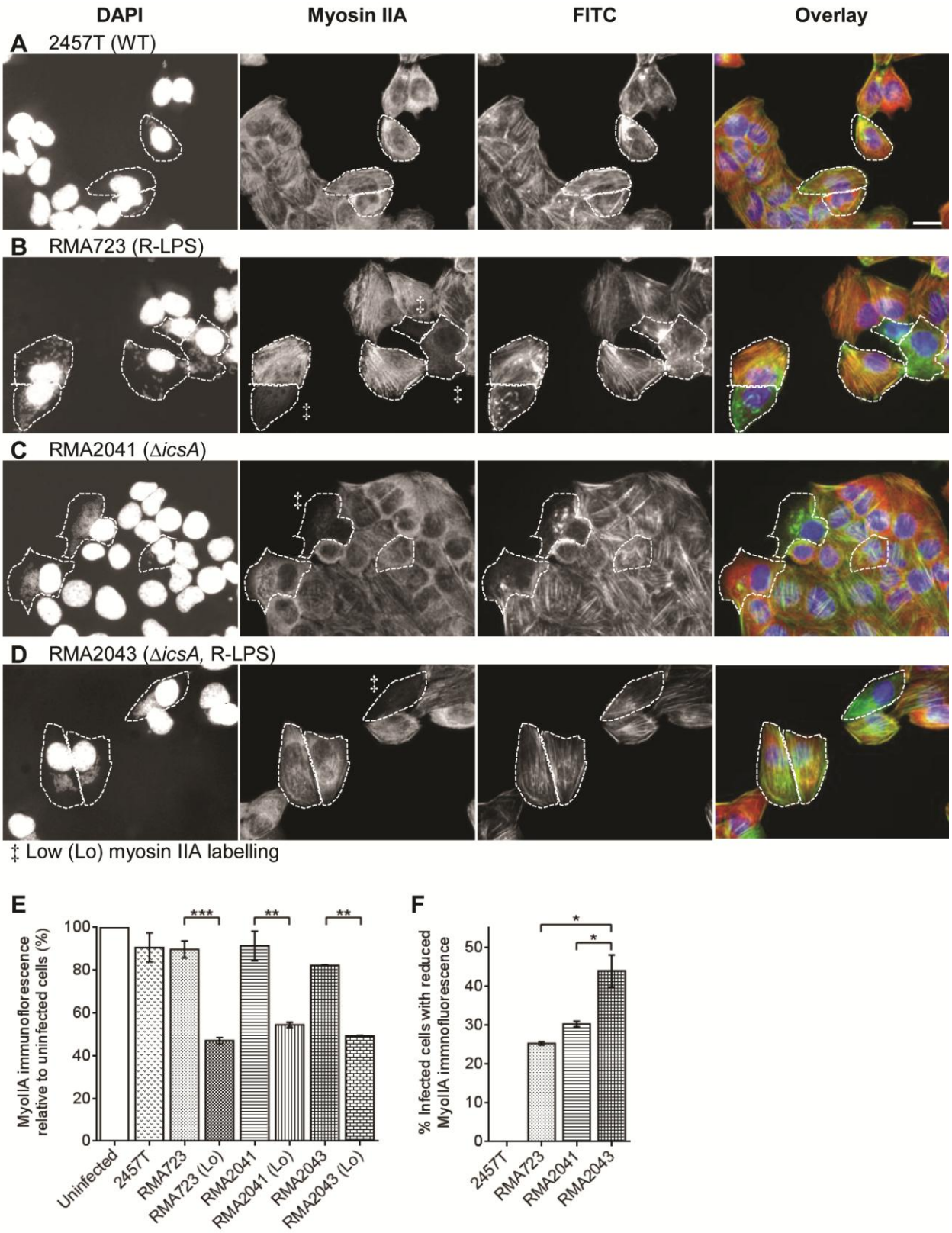
DAPI
Myosin IIA
FITC
Overlay
A 2457T (WT)
B RMA723 (R-LPS)
C RMA2041 (ΔicsA)
D RMA2043 (ΔicsA, R-LPS)
‡ Low (Lo) myosin IIA labelling
E
MyoIIA immunofloresecence relative to uninfected cells (%)
100
80
60
40
20
0
***
**
**
Uninfected
2457T
RMA723
RMA723 (Lo)
RMA2041
RMA2041 (Lo)
RMA2043
RMA2043 (Lo)
F
% Infected cells with reduced MyoIIA immnofluorescence
50
40
30
20
10
0
*
*
2457T
RMA723
RMA2041
RMA2043

743

Fig. 5 Myosin IIA protein levels are significantly reduced when infected with R-LPS and Δ*icsA S. flexneri* strains. HeLa cells were infected with *S. flexneri* strains; (A) 2457T; (B) RMA723 (Δ*rmlD* - R-LPS); (C) RMA2041 (Δ*icsA*); (D) RMA2043 (Δ*icsA* Δ*rmlD*); in an invasion assay as described in the Methods. Bacteria and HeLa nuclei were stained with DAPI (blue), F-actin was stained with FITC-phalloidin (green) and myosin IIA was stained with anti-myosin IIA and Alexa Fluor 594-conjugated secondary antibody (red). Images were taken at 40× magnification. Scale bar = 20 μm. Infected HeLa cells are outlined. Infected HeLa cells with reduced myosin IIA labelling are marked with ‡. (E) The % myosin IIA labelling intensity of infected HeLa cells were compared with uninfected HeLa cells (set at 100%) in each individual image. In instances where infected HeLa cells have marked reduction in myosin IIA immunofluorescence, the infected HeLa cells are grouped into a separate category marked as (Lo = low) of the respective strains. The mean % myosin IIA labelling intensity of infected HeLa cells were determined by measuring ≥ 100 infected HeLa cells in each independent experiment for each category. Data are represented as mean ± SEM of independent experiments (n = 2), analysed with one-way ANOVA ($p < 0.0001$), followed by Tukey's post hoc test (**$p < 0.01$, ***$p < 0.001$). (F) The % infected HeLa cells with low myosin IIA immunofluorescence was determined from the IF images analysed. Data are represented as mean ± SEM of independent experiments (n = 2), analysed with one-way ANOVA ($p < 0.0001$), followed by Tukey's post hoc test (*$p < 0.05$).

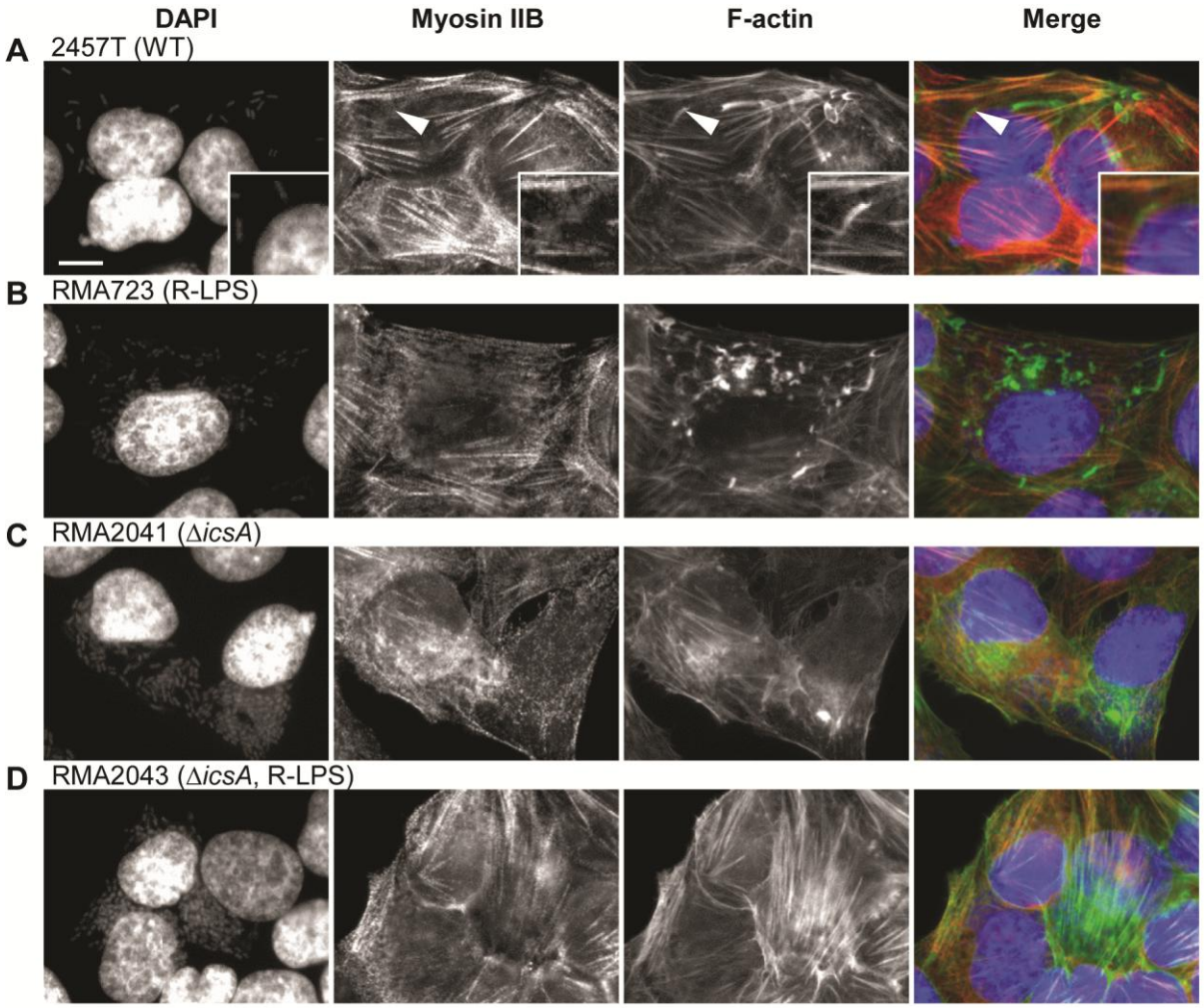

763

764 **Fig. 6 Myosin IIB protein levels are not affected when infected with R-LPS and Δ*icsA S.***
765 ***flexneri* strains.** HeLa cells were infected with *S. flexneri* strains; (A) 2457T; (B) RMA723
766 (Δ*rmlD* - R-LPS); (C) RMA2041 (Δ*icsA*); (D) RMA2043 (Δ*icsA* Δ*rmlD*); in an invasion assay as
767 described in the Methods. Bacteria and HeLa nuclei were stained with DAPI (blue), F-actin was
768 stained with FITC-phalloidin (green) and myosin IIB was stained with anti-myosin IIB and
769 Alexa Fluor 594-conjugated secondary antibody (red). Images were taken at 100× magnification.
770 Scale bar = 10 μm. Arrowheads indicate myosin IIB localisation at the F-actin comet tails. Insert
771 shows 2× enlargement of the indicated region. The experiment was repeated twice and
772 representative images are shown.
773